

---

## Efficient separation and selective Li recycling of spent LiFePO<sub>4</sub> cathode

Yuelin Kong, Lixia Yuan\*, Yaqi Liao, Yudi Shao, Shuaipeng Hao, Yunhui Huang\*

State Key Laboratory of Material Processing and Die and Mold Technology, School of Materials Science and Engineering, Huazhong University of Science and Technology, Wuhan 430074, Hubei, China.

**Correspondence to:** Prof. Lixia Yuan, State Key Laboratory of Material Processing and Die and Mold Technology, School of Materials Science and Engineering, Huazhong University of Science and Technology, 1037 Luoyu Road, Wuhan 430074, Hubei, China. E-mail: [yuanlixia@hust.edu.cn](mailto:yuanlixia@hust.edu.cn); Prof. Yunhui Huang, State Key Laboratory of Material Processing and Die and Mold Technology, School of Materials Science and Engineering, Huazhong University of Science and Technology, 1037 Luoyu Road, Wuhan 430074, Hubei, China. E-mail: [huangyh@hust.edu.cn](mailto:huangyh@hust.edu.cn)

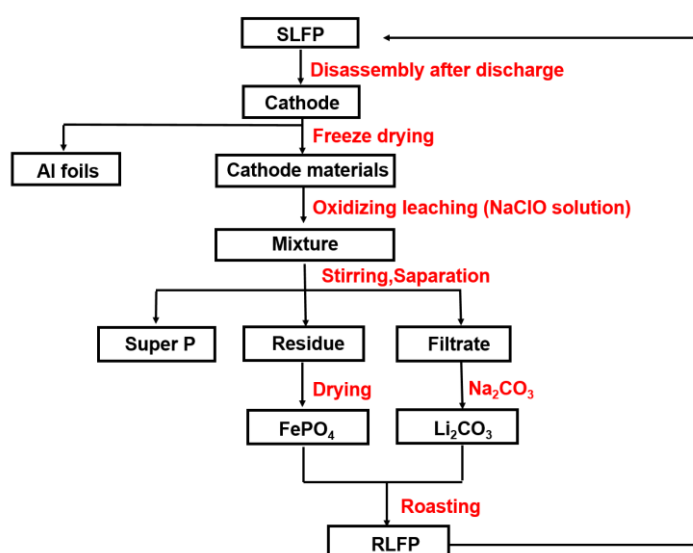


Figure S1 Process diagram of recycling spent LFP cathode materials

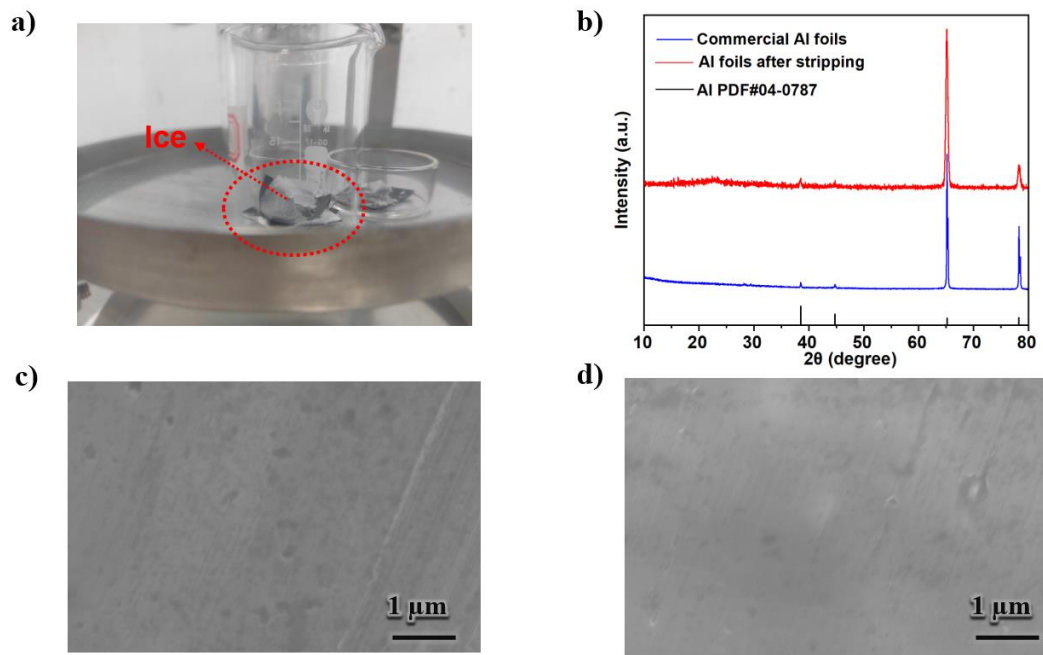


Figure S2 (a) digital photos of SLFP cathode under freeze drying. (b) XRD characterization patterns of Al foil after stripping and commercial Al foil. (c and d) SEM images of recycled Al foil and commercial Al foil.

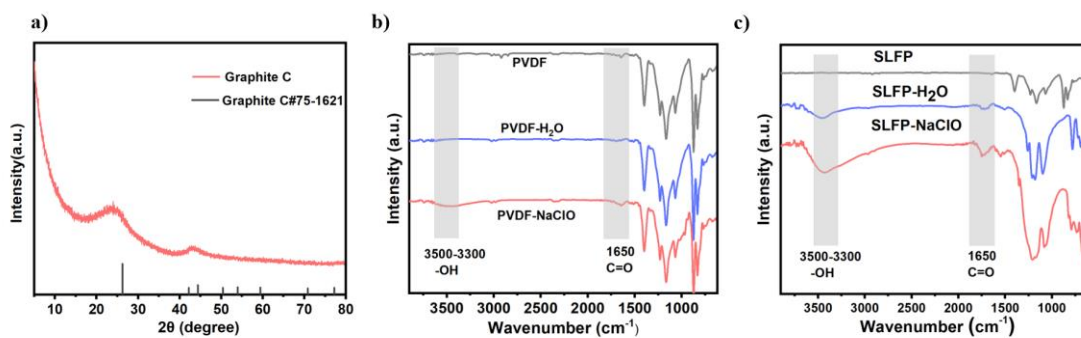


Figure S3 (a) XRD characterization patterns of recycled super P. (b) FTIR spectra of the pristine PVDF reacting with NaClO or H<sub>2</sub>O. (c) FTIR spectra of SLFP layer reacting with NaClO or H<sub>2</sub>O.

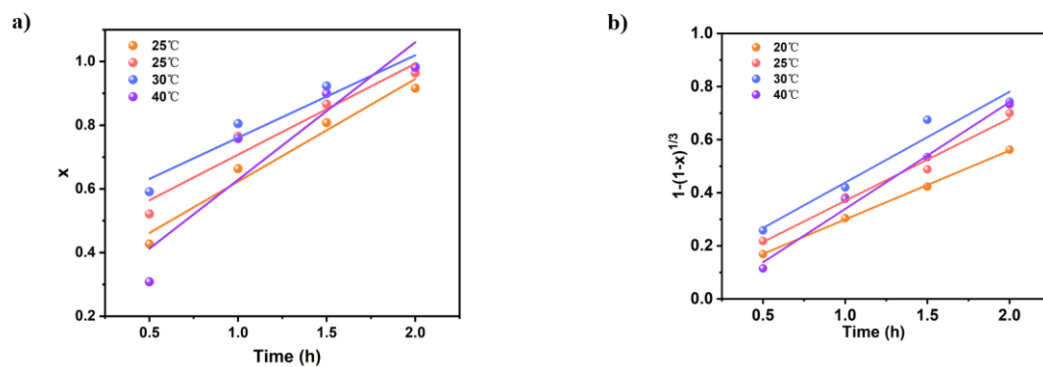


Figure S4 Kinetics fitting diagram at different temperature for (a) external diffusion model and (b) chemical reaction model.

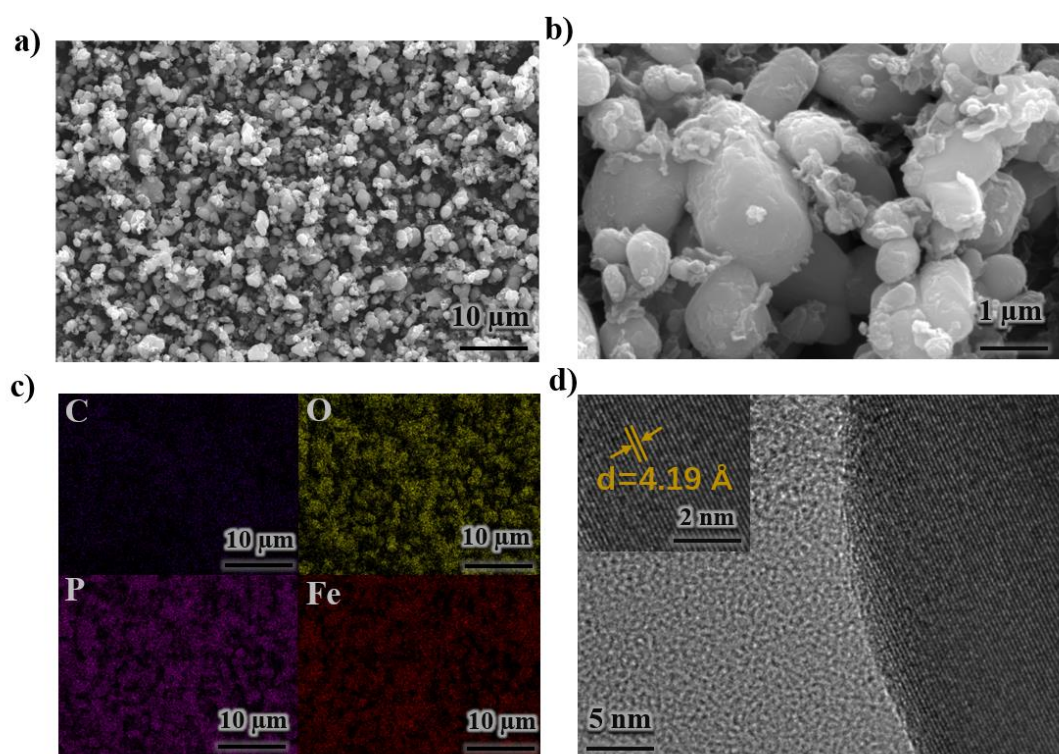


Figure S5 (a, b) SEM images of CLFP. (c) EDS mapping of CLFP (corresponding to Fig.S5a). (d) HRTEM images of CLFP.

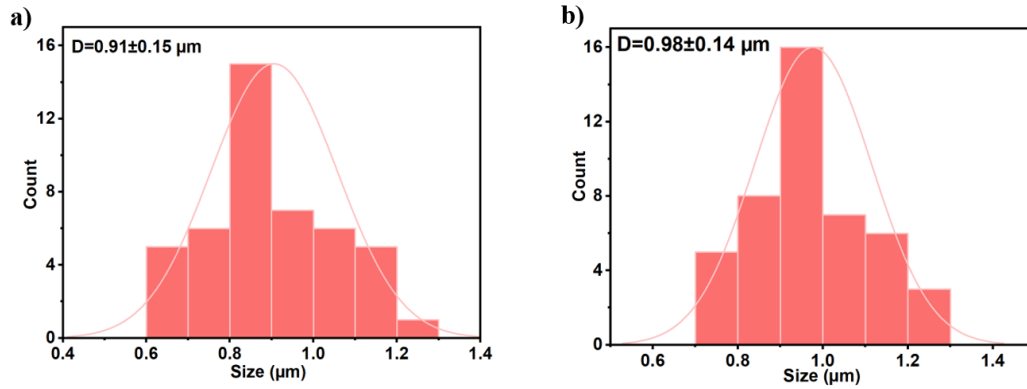


Figure S6 (a, b) The particle size distributions of RLFP and CLFP

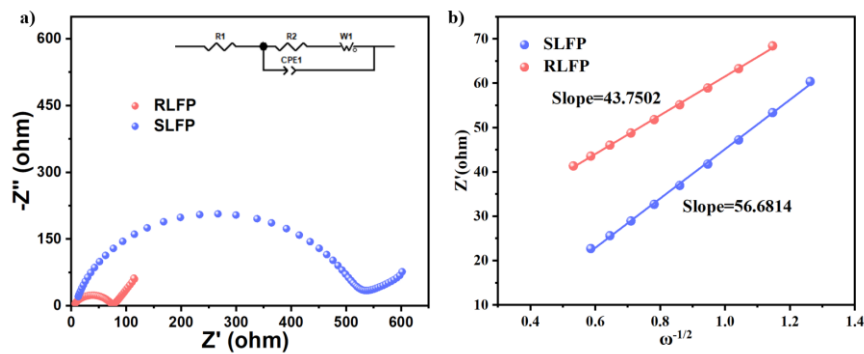


Figure S7 (a) Nyquist plots of SLFP and RLFP (0.01 Hz-100 kHz). (b) The linear fitting curves of  $Z' \sim \omega^{-1/2}$  of SLFP and RLFP.

Table S1 The content of each element in the SLFP cathode materials.

Element	Li	Fe	P	Al
Content (wt.%)	3.46	26.67	14.85	0.03

Table S2 The concentration of each element in the leaching solution of the peeling SLFP treated by NaClO and ultrapure water.

Element	Li	Fe	P	Al
Concentration (mg L <sup>-1</sup> )				
NaClO	1062.48	3.06	112.80	0.08
Ultrapure water	3.65	2.97	56.30	0.06

Table S3 The leaching result of Li<sup>+</sup> at different temperatures and different time.

Leaching efficiency (%)	Times (h)					
	0.5	1	1.5	2	2.5	3
Temperature (°C)						
20	42.7%	66.3%	80.8%	91.6%	90.4%	89.6%

25	52.1%	76.5%	86.6%	96.4%	88.8%	88.3%
30	59.1%	80.5%	92.3%	98.3%	98.2%	98.1%
40	30.8%	75.8%	89.9%	98.1%	77.6%	78.5%

Table S4 The kinetics fitting data of x at different temperatures varies with time.

Kinetics fitting data	Times (h)					
	0.5	1	1.5	2	2.5	3
Temperature (°C)						
20	0.427	0.663	0.808	0.916	0.904	0.896
25	0.521	0.765	0.866	0.964	0.888	0.883
30	0.591	0.805	0.923	0.983	0.982	0.981
40	0.308	0.758	0.899	0.981	0.776	0.785

Table S5 The kinetics fitting data of  $1-2/3x-(1-x)^{2/3}$  at different temperatures varies with time.

Kinetics fitting data	Times (h)					
	0.5	1	1.5	2	2.5	3
Temperature (°C)						
20	0.026	0.074	0.129	0.198	0.097	0.094
25	0.041	0.109	0.161	0.248	0.176	0.172
30	0.055	0.127	0.204	0.279	0.277	0.275
40	0.012	0.106	0.184	0.275	0.114	0.118

Table S6 The kinetics fitting data of  $1-(1-x)^{1/3}$  at different temperatures varies with time.

Kinetics fitting data	Times (h)					
	0.5	1	1.5	2	2.5	3
Temperature (°C)						
20	0.169	0.304	0.423	0.562	0.357	0.350
25	0.218	0.383	0.488	0.700	0.518	0.511
30	0.258	0.420	0.575	0.734	0.738	0.733
40	0.115	0.377	0.534	0.733	0.393	0.401

Table S7 The fitting data of different kinetic models at different leaching temperatures.

Kinetic models	20°C		25°C		30°C		40°C	
	Slope	R <sup>2</sup>	Slope	R <sup>2</sup>	Slope	R <sup>2</sup>	Slope	R <sup>2</sup>
External diffusion	0.322	0.968	0.286	0.942	0.259	0.933	0.197	0.863
Internal diffusion	0.114	0.993	0.135	0.990	0.149	0.999	0.173	0.999
Chemical reaction	0.260	0.999	0.310	0.984	0.322	0.980	0.402	0.984

Table S8 The data from calculating lithium-ion diffusion coefficients based the lines of  $Z' \sim \omega^{-1/2}$

---

for RLFP and SLFP

---

	RLFP	SLFP
Slope	43.7502±0.4511	55.6814±0.6809
Intercept	17.8149±0.3741	-10.4908±0.6251
R <sup>2</sup>	0.9993	0.9990
D <sub>Li</sub> (cm <sup>2</sup> s <sup>-1</sup> )	1.62*10 <sup>-15</sup>	9.98*10 <sup>-16</sup>

---

Text S1 Principle and calculation formula of leaching kinetics

In the process of leaching by hydrometallurgy, the reaction principle between solid reactants and leaching solution confirms to be typical shrinking core models. According to this theory, the chemical reaction steps mainly occur at the interface of the unreacted nucleus, and the leaching process gradually diffuses from the external solution to the unreacted particles, while the diffusion process of the leaching solution is the opposite. The leaching steps are as follows:

- (1) The leaching agent diffuses through the solution to the surface of the solid reactant particles, represented as external diffusion step.
- (2) The leaching agent passes through the solid product layer to the surface of the unreacted nucleus, represented as internal diffusion step.
- (3) The leaching agent reacts on the surface of the solid reactant, represented as chemical reaction step.
- (4) The leachate reaches the surface of the solid reactant particles from the reaction interface through the solid product layer.
- (5) The leachate diffuses from the surface of the solid reactant particles back into the solution.

When external diffusion, internal diffusion and chemical reaction are respectively the rate control steps of leaching process, the leaching kinetics equations are shown in equations (1) - (3).

$$x = k_1 t \quad (1)$$

$$1 - 2/3x - (1 - x)^{2/3} = k_2 t \quad (2)$$

$$1 - (1 - x)^{1/3} = k_3 t \quad (3)$$

Where x represents the leaching efficiency of Li (%), k<sub>1</sub>, k<sub>2</sub>, k<sub>3</sub> represent the reaction rate constants in each situation (min<sup>-1</sup>), t represents the oxidation time (min).

Text S2 Calculation of activation energy of chemical reaction by Arrhenius equation

The equation is shown below:

$$k = A e^{-\frac{E_a}{RT}} \quad (4)$$

$$\ln k = \ln A - \frac{E_a}{RT} \quad (5)$$

Where k, A, E<sub>a</sub>, R, and T represent the reaction rate constant (min<sup>-1</sup>), pre-exponential factor; apparent activation energy (kJ mol<sup>-1</sup>), universal gas constant (8.314 J K<sup>-1</sup> mol<sup>-1</sup>), absolute temperature (K), respectively.

---

Text S3 Electrochemical impedance spectroscopy (EIS)

The semi-circle part and the straight part of the Nyquist plot represent the high frequency region and the low frequency region, respectively. The low frequency region line is equivalent to the lithium-ion diffusion impedance, and the lithium-ion diffusion coefficient can be obtained by slope calculation. Equations are as follows:

$$Z' = K + \sigma\omega^{-1/2} \quad (6)$$

$$D_{\text{Li}} = \frac{R^2 T^2}{2n^2 F^4 A^2 C^2 \sigma^2} \quad (7)$$

In Equation (6),  $Z'$  represents the real part of impedance,  $\sigma$  represents the Warburg coefficient,  $\omega$  is the angular frequency. In Equation (7),  $D_{\text{Li}}$  represents the lithium-ion diffusion coefficients ( $\text{cm}^2 \text{s}^{-1}$ ),  $R$  represents gas constant ( $8.314 \text{ J mol}^{-1} \text{ K}^{-1}$ ),  $T$  represents the absolute temperature (K),  $n$  represents the electron transfer number of  $\text{LiFePO}_4$  molecules during lithium intercalation (1.0),  $F$  represents Faraday constant ( $96485 \text{ C mol}^{-1}$ ),  $A$  represents the surface area of the electrode ( $0.50 \text{ cm}^2$ ),  $C$  represents the concentration of  $\text{Li}^+$  in LFP ( $2.28 \times 10^{-2} \text{ mol cm}^{-3}$ ),  $\sigma$  represents the slope of  $Z' \sim \omega^{-1/2}$ .